JOURNAL OF MATERIALS SCIENCE **35** (2000) 2069–2077

Fracture toughness of high-chromium white irons: Influence of cast structure

C. P. TABRETT
CW Pope and Associates Pty Ltd, Box 96, Hunter Region Mail Centre, NSW 2310, Australia
E-mail: tabrec@cwpope.com.au

I. R. SARE
CSIRO Manufacturing Science and Technology, Private Bag 33, Clayton South MDC, VIC 3169, Australia

The fracture toughness of two high-chromium white iron alloys in the as-cast condition has been investigated. Fracture toughness test pieces were extracted at various orientations relative to the columnar macrostructure. The toughness of a 27 Cr white iron alloy was very sensitive to orientation, and the toughness was much larger when the crack propagated in a direction perpendicular to the long dimension of the eutectic carbides. The toughness of the 15-3 Cr-Mo white iron was insensitive to the orientation. The different fracture behaviour of the two alloys was related to the anisotropy of the eutectic carbide structures in the as-cast material. The limitations in applying quantitative data on the eutectic carbide structure to models of fracture toughness in white iron alloys were illustrated.

1. Introduction

The excellent abrasion resistance of high-chromium white iron alloys is due primarily to the presence of hard primary and/or eutectic carbides in the microstructure [1, 2]. These carbides, however, also play a critical role in the fracture behaviour of white iron alloys, and the toughness deteriorates as the proportion of carbides in the structure increases [3]. Since a high proportion of carbides in the structure are required to maximise the abrasion resistance, many researchers have sought to improve the toughness through modifications to the carbide structure [4, 5]. The carbide attributes which have been manipulated in an attempt to improve toughness include volume fraction [3, 6, 7], carbide size [5] and inter-carbide spacing, and carbide morphology and shape [4]. These studies have found, with varying degrees of success, that the toughness of high-chromium white irons may be improved by decreasing the proportion of carbides in the structure, decreasing the carbide size, increasing the inter-carbide spacing, and globularising the carbide shape.

For many components produced from white iron alloys, a columnar grain structure is formed. In this columnar structure, the eutectic carbides are usually aligned so that the long axis of the carbide rods is parallel with the direction of heat extraction (i.e. perpendicular to the cast surface). Laird and Dogan [8] have shown recently that the notched impact fracture energy of high-chromium white irons, measured using a single-blow drop-weight test [9], is influenced by the macrostructure of the cast material. The macrostructure may be determined by such factors as the casting geometry, presence of chills, the pouring superheat and the alloy composition. Further, metallographic examination has suggested that many aspects of the carbide network (e.g., carbide size, inter-carbide spacing, morphology) are different for each orientation relative to the columnar structure [10]. The question arises, then, as to how the fracture behaviour and measured fracture toughness vary with orientation relative to the cast columnar structure. This study examines the fracture behaviour and fracture toughness of two high-chromium white iron alloys (15-3 Cr-Mo and 27 Cr [11]) in the as-cast condition. Fracture toughness specimens were extracted from the cast material for three orientations of the expected crack growth direction relative to the columnar structure. The chevron-notched, short-bar toughness test was used to measure fracture toughness [12]. Metallographic observations and quantitative analysis of the carbide structure were applied to existing toughness models for white irons and used to interpret the observed fracture behaviour.

2. Materials and test methods

Two high-chromium white iron alloys were melted in an induction furnace and cast into sodium silicate—CO_2 bonded sand moulds as blocks of $200\times75\times22$ mm^3. The pouring temperature for both alloys was approximately 1450°C. The chemical compositions of the alloys, determined using optical emission spectroscopy, are given in Table I. The bulk hardness of each alloy is also given in Table I [10]. The macrostructure formed in the cast blocks was columnar and is represented in Fig. 1.

TABLE I Chemical composition (wt.%) and bulk hardness (HV_{30}) of high-chromium white iron alloys

Alloy	C	Cr	Si	Mo	Mn	Ni	Fe	Hardness (HV_{30})[a]
27 Cr	2.5	28.3	0.7	—	0.8	0.2	rem	519 ± 14
15-3 Cr-Mo	3.1	14.8	0.6	3.2	0.6	—	rem	507 ± 15

[a]Mean $\pm$ standard deviation

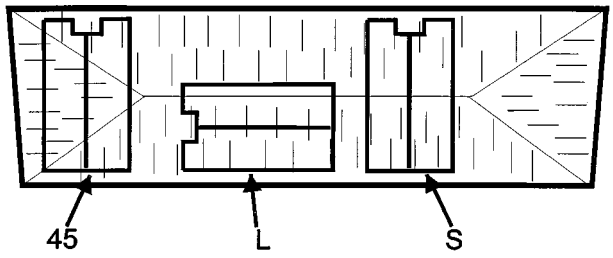

Figure 1 Schematic illustration of the cross-sectional macrostructure of the cast blocks of as-cast 27 Cr and 15-3 Cr-Mo white iron alloys. The location of the short-bar fracture toughness test pieces, defined as orientations S, L and 45°, is also shown.

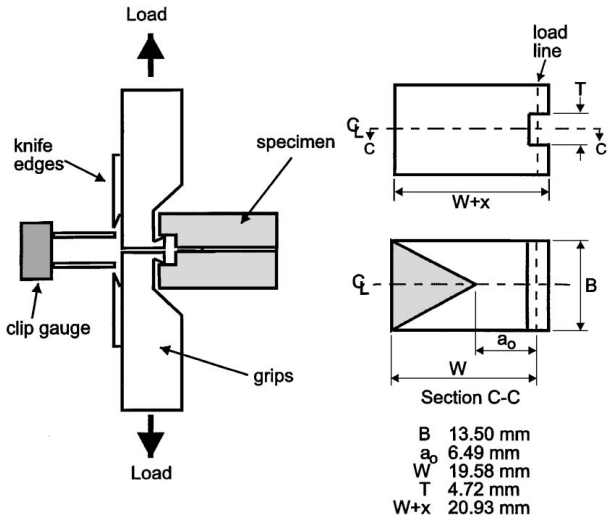

Figure 2 Loading arrangement and the dimensions of short-bar fracture toughness test pieces.

Short-bar fracture toughness test pieces were machined from the cast blocks to the dimensions shown in Fig. 2. The orientation of the test pieces was chosen so that the expected crack growth direction (the plane of the chevron-notch) was parallel (S), perpendicular (L) or at an angle (45°) to the growth direction of the columnar structure. The location of the test pieces in the cast blocks is shown schematically in Fig. 1. All fracture toughness tests were carried out using a servo-hydraulic load frame under displacement control. A clip gauge mounted on knife edges across the loading grips was used to monitor displacement. The loading arrangement is illustrated schematically in Fig. 2. The displacement rate was 0.25 mm/min, and the fracture toughness was determined by *maximum load analysis* [12]. Due to the elastic behaviour of high-chromium white irons, the *maximum load* technique has been shown to yield the same results as the unloading technique that incorporates a plasticity criterion [13]. The maximum load (P_m) is measured, and the short-bar fracture toughness ($K_{I\nu m}$) determined according to the equation:

$$K_{I\nu m} = \frac{P_m Y^*}{B\sqrt{W}} \quad (1)$$

Where B = specimen width (normally 13.5 mm), W = specimen length to load line, Y^* = compliance constant (= 25.11 for geometry used [12]).

Following testing, the fracture surfaces were examined in the scanning electron microscope (SEM).

Metallographic characterisation of the eutectic carbides in the plane of the chevron-notch for each test piece orientation was performed (Fig. 1). The cast blocks were sectioned using a water-cooled abrasive cut-off wheel, mounted in bakelite, and ground and polished using conventional metallographic techniques to a final 3 μm diamond finish. The samples were etched in Marble's reagent for up to 6 minutes. Quantitative analysis of the eutectic carbides in each alloy and for each orientation was carried out using image analysis [10]. Image analysis requires high contrast between the phases to be discriminated (in this case, the carbides from the matrix). Etching in Marble's reagent darkened the matrix, while the eutectic carbides were not attacked, and remained white. This etching produced sufficient difference in the *grey level* of each phase to discriminate using image analysis. The area fraction, average size, number of carbides per unit area and aspect ratio of the cross-section of the eutectic carbides was determined from 50 fields for each alloy and orientation [10]. The size is defined as the diameter of a circle of equal area to the carbide.

3. Results

3.1. Variability of short-bar fracture toughness test

Variability of six replicate tests of the 27 Cr alloy in orientation S is given in Table II. The mean $K_{I\nu m}$ was 26.6 MPa$\sqrt{}$m, while the coefficient of variation was approximately 10%. This suggests that the repeatability of this test, for the S orientation of the 27 Cr alloy, is good, and comparable with that obtained with other materials [14].

3.2. Effect of orientation on fracture toughness

The fracture toughness results for the high-chromium white iron alloys, 15-3 Cr-Mo and 27 Cr, in the S, L and 45° orientations are given in Table III. The maximum load and $K_{I\nu m}$ calculated according to Equation 1 are presented. The $K_{I\nu m}$ values for the L orientation are not strictly valid results owing to extreme crack deviation from the notch plane. Nevertheless, it is evident that for the 27 Cr alloy the fracture toughness is lowest

TABLE II Repeatability of short-bar fracture toughness test

Alloy	$K_{I\nu m}$ (MPa $\sqrt{}$m)						mean $\pm$ sdev
27 Cr (s)	25.9	25.2	31.6	24.0	25.5	27.5	26.6 ± 2.7

TABLE III Maximum load (P_m) and apparent short-bar fracture toughness (K_{Ivm}) for various white iron alloys and orientations

Alloy	Orientation	Maximum load, P_m (kN)	Apparent fracture toughness, K_{Ivm} (MPa $\sqrt{m}$)[a]	
27Cr	S	1.95	25.9	(26.6)
		1.89	25.2	
		2.37	31.6	
		1.79	24.0	
		1.85	25.5	
		2.04	27.5	
	L	4.80	64.1	(57.3)
		4.14	54.7	
		4.00	53.2	
	45°	3.24	43.4	(42.1)
		3.05	40.7	
	S	2.01	26.9	(28.7)
		2.25	30.4	
	L	2.45	32.9	(32.9)
		2.48	32.8	
	45°	2.43	32.3	(29.0)
		1.80	25.7	

[a]Mean values given in parentheses.

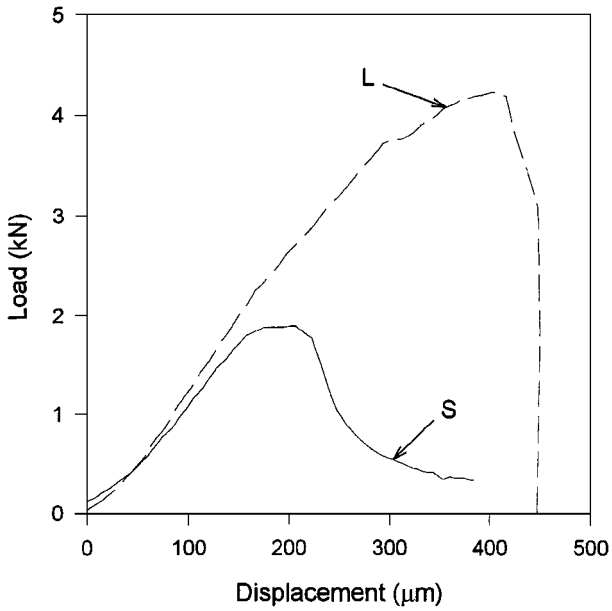

Figure 3 Load-displacement traces for the L and S orientation samples of the 27 Cr white iron alloy.

in the S orientation. The toughness values for the 45° orientation are higher than those for the S orientation, while the apparent toughness of the L Orientation is much greater. Indeed, the apparent toughness values of 53–64 MPa$\sqrt{m}$ for the latter far exceed the maximum fracture toughness data for high-chromium white irons quoted in the literature [6, 13]. The load-displacement traces for the L and S oriented samples of the 27 Cr alloy are given in Fig. 3, and highlight the greater resistance to fracture of the L orientation.

For the 15-3 Cr-Mo alloy, there appeared to be very little difference in the fracture toughness for each orientation. The toughness values for the L and 45° orientations appeared to be slightly higher than that of the S orientation. However, given the limited number of tests performed, this difference was not considered to be significant.

Macrographs of the fractured specimens in the S, 45° and L orientations are given for the 27 Cr and 15-3 Cr-Mo white irons in Fig. 4. The fracture path for the S orientation in the 27 Cr alloy (Fig. 4a) is relatively flat, and coplanar with the chevron notch. The L orientation for this alloy (Fig. 4b), however, shows severe macroscopic deviation of the crack. At final fracture, the crack path is perpendicular to the plane of the chevron notch. This phenomenon was observed for all three test pieces at this orientation. The 45° samples of the 27 Cr alloy (Fig. 4c) showed an initial region of flat, coplanar crack growth. However, as the crack length increased, the crack deviated from the notch plane at an angle of up to 30°. The fracture paths for the 15-3 Cr-Mo alloy (Fig. 4d–f) were all macroscopically flat. No crack deviation, even for the samples in the L orientation, was observed.

Examination in the SEM revealed that the dominant feature on the fracture surface of the S orientation of the 27 Cr alloy was long carbides aligned in the direction of crack propagation, as shown in Fig. 5a. The proportion of eutectic carbides on the surface exceeds the volume fraction of the bulk material. The rounded, featureless nature of the eutectic carbides on the surface suggests that fracture was predominantly along the carbide-matrix interfaces. Small regions of matrix appear on the fracture surface, and exhibit features of cleavage fracture.

The fracture surface of the L orientation of the 27 Cr alloy was characterised by two separate regions. The initial, stable crack growth region, which was macroscopically flat, was microscopically rough, with undulations. A micrograph of this surface is given in Fig. 5b. Fracture appeared to have occurred along the carbide-matrix interface, but the carbides on the fracture surface were much smaller (<20 μm). Larger regions of matrix material were present, with cleavage again appearing to be the predominant mode of failure. As the crack length increased, and the crack began to deviate macroscopically, the appearance of the fracture surface changed. As may be seen in Fig. 5c, the length of the carbides on the surface increased to between 50 and 100 μm, with 'steps' between the carbide lengths. The length of the carbides on the surface was not as long as those for the fractured surface of the S orientation. The proportion of carbides on the fracture surface increased as the crack length increased and the crack deviated. The fracture surface for the 27 Cr alloy in the 45° orientation is shown in Fig. 5d. The length of the carbides on this surface was 60–100 μm, with steps between each carbide length.

The fracture surfaces for the 15-3 Cr-Mo alloy produced similar trends to those observed in the 27 Cr alloy, although the difference between the orientations was not as pronounced as for the 27 Cr white iron. For the 15-3 Cr-Mo in the S orientation, the fracture surface, shown in Fig. 6a, showed regions of aligned eutectic carbides of up to 200 μm in length. Fracture appeared to be predominantly along the carbide-matrix interface. The amount of matrix on the fracture surface was greater than for the 27 Cr alloy in the S orientation. The fracture surface for the 15-3 Cr-Mo alloy in the L orientation showed fewer examples of aligned

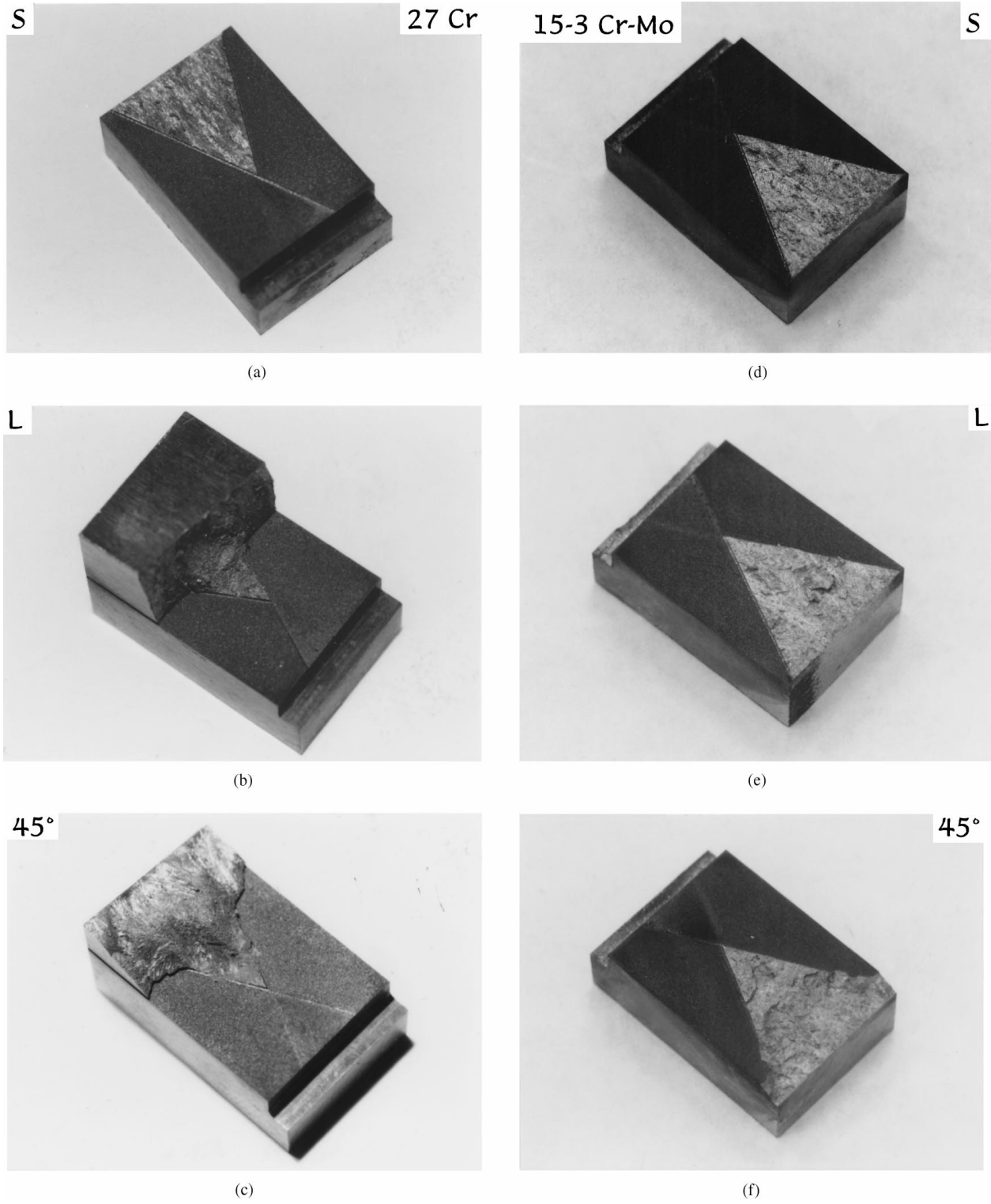

Figure 4 Macrographs of fractured specimens for the 27 Cr and 15-3 Cr-Mo white iron alloys.

carbides, and the lengths of the carbides on the fracture surface were generally less than 75 μm. The surface, shown in Fig. 6b, also contained a greater proportion of matrix than for the S oriented samples. For both alloys and orientations, the matrix appeared to fail by a quasi-cleavage mechanism, as illustrated in Fig. 6c.

3.3. Analysis of carbide structure

Quantitative analysis of the eutectic carbides in the plane of the chevron notch for each orientation was performed using an image analysis technique. Polished metallographic samples of both alloys were used. The results from this analysis are given in Table IV. It can be seen that the area fraction of eutectic carbides on the notch plane of sample orientation does not differ significantly. The equivalent particle diameter also appears relatively insensitive to orientation, although the L orientation does appear to have slightly smaller carbide particles for both alloys. A difficulty in using particle diameter or size as a measure is the large scatter in the measured results. This is evident from the large standard

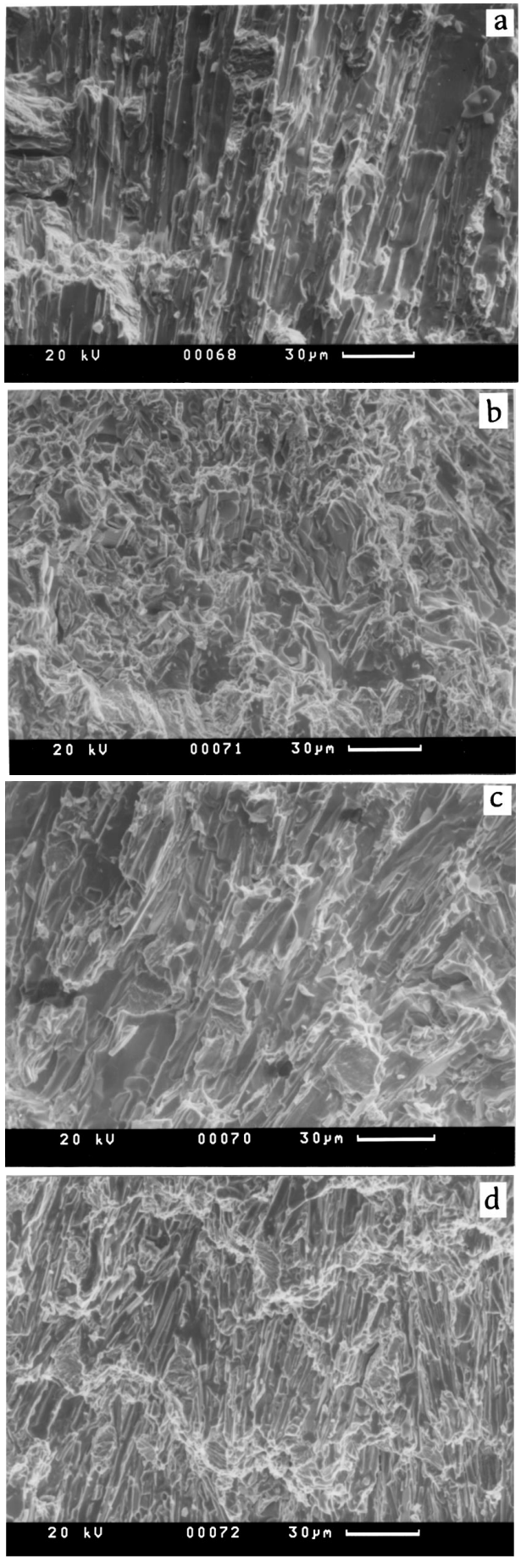

Figure 5 SEM micrographs of fracture surface of the 27 Cr white iron alloy in (a) S orientation, (b) L orientation (initial crack growth region), (c) L orientation (deflected crack growth region) and (d) 45° orientation (deflected crack growth region). A 'step' from carbide to carbide is arrowed in (a).

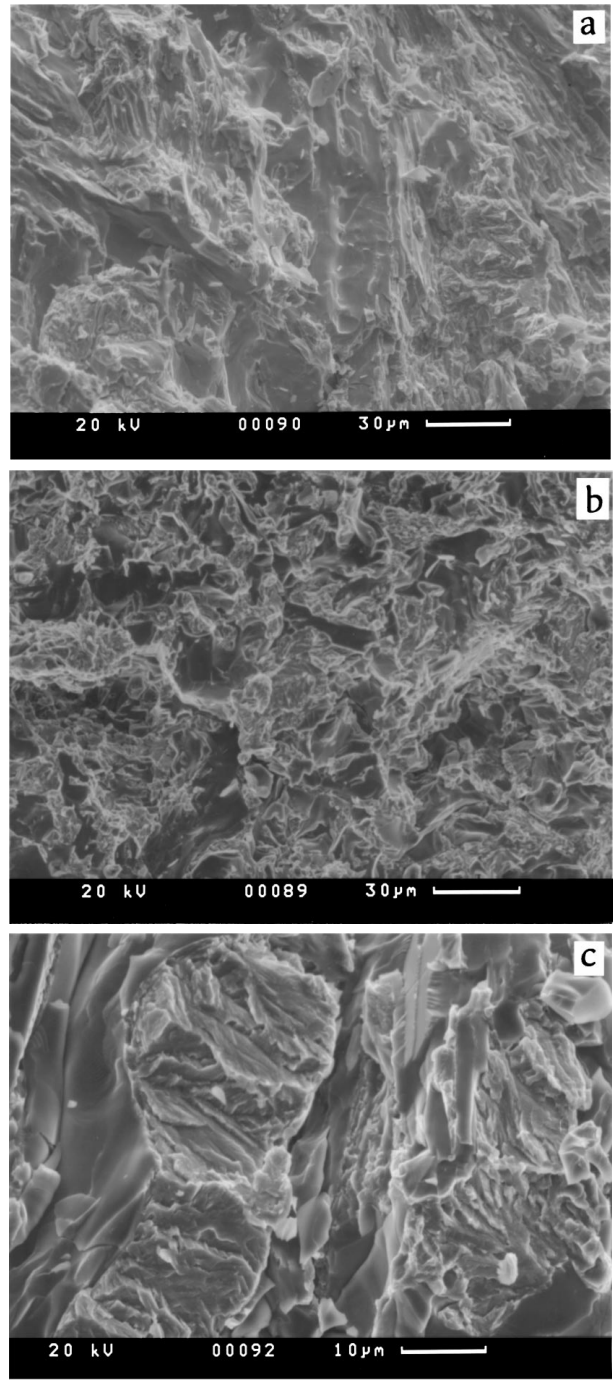

Figure 6 SEM micrographs of fracture surface of the 15-3 Cr-Mo white iron alloy in (a) S orientation, (b) L orientation, and (c) illustration of matrix fracture by quasi-cleavage.

deviation for the particle diameter results, which led to values of the coefficient of variation of 30–40%. The measurement of number of particles per unit area varies significantly with orientation, particularly for the 27 Cr alloy. As the area fraction of eutectic carbides is similar for each alloy, an increase in the number of particles per unit area is an indicator of a structure containing smaller carbide particles. This is reflected to a limited degree in the particle diameter results, but again, the large scatter in these measurements hinders their interpretation.

The theoretical area fraction may be calculated from the measured particle diameters, and differs from the measured area fraction. This is due to skew to the left in the distribution of equivalent particle diameter

TABLE IV Quantitative analysis of eutectic carbides in high-chromium white iron alloys[a]

Alloy	Orientation	Area fraction[a] (%)	Equivalent Particle diameter[a] (μm)	No. of carbide particles/mm^2	Aspect ratio[a]
27Cr	L	23.6±2.2	4.6±1.7	8185	2.2±0.9
	S	22.3±2.1	5.6±1.9	3440	3.1±1.8
15-3 Cr-Mo	L	21.9±2.1	5.4±2.0	3300	2.2±0.9
	S	23.7±2.3	6.5±2.2	1985	2.4±1.2

[a]Values are mean ± standard deviation.

measurements. This skew was observed for both alloys, and reduced the apparent difference in equivalent particle diameter between the various orientations of the 27 Cr alloy.

The mean aspect ratio for the eutectic carbides in the 27 Cr alloy was higher in the S orientation than for the L orientation. In contrast, the results for the aspect ratio of the eutectic carbides in the 15-3 Cr-Mo were similar for both the L and S orientation. For both alloys, the measurement of the aspect ratio yielded a coefficient of variation of between 40 to 60%. This is a reflection of the heterogeneity of the carbide structure in high-chromium white irons.

The nature of the eutectic carbide structure was examined qualitatively using SEM observation of material that had been deep-etched. The deep-etching technique, which involved immersion in an aqua regia solution for up to 3 minutes, dissolves the iron matrix. When examined in the SEM the three-dimensional characteristics of the carbide structure become apparent [1, 15]. Samples of the 27 Cr and 15-3 Cr-Mo alloys were sectioned, metallographically ground and polished, then deep-etched in the aqua regia solution. The deep-etched structures are shown in Fig. 7. Two perpendicular faces, corresponding to the planes S and L, are shown for each alloy. The eutectic carbides appear rod-like in the 27 Cr alloy (Fig. 7a), and mostly blade-like for the 15-3 Cr-Mo alloy (Fig. 7b). In the 27 Cr alloy, the eutectic carbides appear strongly directional, with the long axis of the carbide rods aligned in the S orientation. The L plane, however, appears to cut the carbide rods perpendicular to the long dimension. The micrograph of the deep-etched 15-3 Cr-Mo alloy also reveals the three-dimensional mature of the eutectic carbides. However, the anisotropy of the eutectic carbide structure was much less than that observed in the 27 Cr alloy.

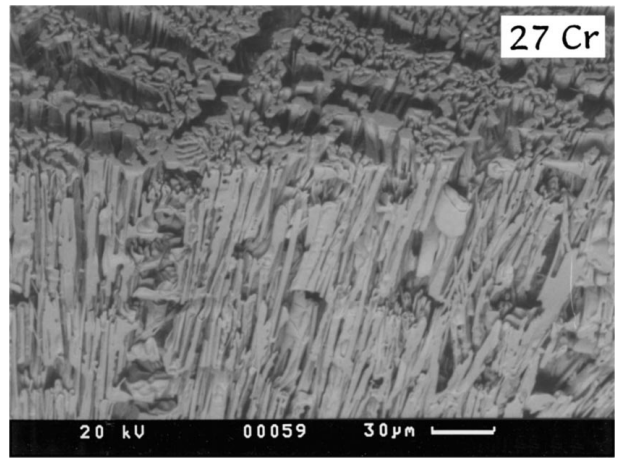

(a)

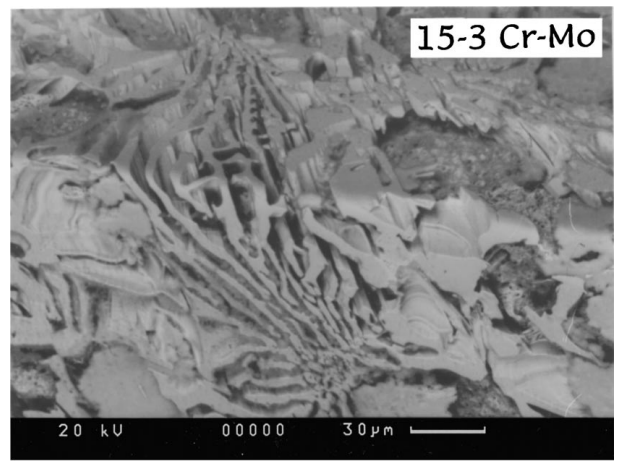

(b)

Figure 7 SEM micrographs of deep-etched 27 Cr and 15-3 Cr-Mo white iron alloys.

4. Discussion

The variability of the replicate tests on the 27 Cr white iron alloy in the S orientation was less than 10%. The appropriate standard for the short-bar test, ASTM E1304 [12], makes no mention of an 'acceptable' variability, but the results of a study of the toughness of various ferrous and non-ferrous alloys is given. The coefficient of variation from these tests varied from about 3 to 15%, and as such, the results of the present work would appear acceptable. This suggests that even for a heterogeneous material such as a high-chromium white iron alloy, good repeatability may be obtained with the short-bar test for a given alloy and orientation. Slightly better repeatability has been obtained with this test for high-chromium white iron alloys by other researchers [13, 16]. Tests by Elwell [13] on an as-cast 28 Cr white iron yielded a coefficient of variation of 4%, while Biner *et al.* [16], who measured the toughness of a range of white iron alloys, found a coefficient of variation of less than 4%. Obviously, the repeatability that may be obtained will depend not only on the alloys and conditions tested, but also the fixtures and measuring devices used (e.g., clip gauge, load cell) [12]. The mean value of ($K_{\mathrm{I}\nu\mathrm{m}}$) determined for the 27 Cr alloy in the S orientation (26.6 MPa$\sqrt{\mathrm{m}}$) is comparable to previous results for similar alloys [13].

The fracture toughness results for the 27 Cr alloy revealed a very strong effect of orientation. The validity of the fracture toughness results for the L orientation is limited, given the gross deflection of the crack. However, the maximum loads measured (P_{m}) for each

indicate a much greater resistance to fracture in the L orientation compared to the S and 45° orientations. Microscopic observations from the fracture surface revealed a significant difference in interaction between the crack path and microstructure. For the S orientation, the large eutectic carbide rods were favourably aligned for the crack to propagate in the plane of the chevron notch along the carbide-matrix interface. Due to the strongly directional nature of the eutectic carbides in the 27 Cr alloy, a large number of carbides were favourably aligned. The crack was able to propagate with little microscopic roughness. The predominance of eutectic carbides on the fracture surface of high-chromium white irons, as found in some of the fracture surfaces of the 27 Cr alloy in this study, has been observed consistently by other researchers [3].

The 45° orientation in the 27 Cr alloy also fractured primarily along the carbide-matrix interfaces. For this orientation, however, as the crack length increased, the carbide rods were no longer coplanar, but rather were at an angle relative to the notch plane. The crack deflected so as to follow the carbide-matrix interface, but a series of steps on the fracture surface suggest that it was favourable for the crack to be closer to the notch plane. Consequently, the crack would 'jump' from one carbide-matrix interface to another, producing the step-like features observed on the fracture surface. It is possible that this macroscopic crack tortuosity, contributed to the improvement in toughness of this orientation compared to the S orientation. It becomes obvious from Fig. 1 that the extent of this phenomenon in the 45° orientation would be dependent on the precise location of the test piece relative to the macrostructure. This sensitivity to location may have led to the greater scatter observed for the 45° orientation.

For the 27 Cr alloy in the L orientation, large favourably aligned carbide rods are no longer present in the notch plane. The crack in this orientation appears to continue to propagate partly along the carbide-matrix interface, but also through the carbides in a direction perpendicular to their long dimension. This produces much greater microscopic roughness on the fracture surface. The growing crack also encounters more areas of matrix material, which would be expected to produce toughening. As the crack grows, and the load increases, it appears that the stress field associated with the crack tip produces delamination-type cracks to appear along the carbide-matrix interfaces of the carbide rods at 90° to the notch plane. At some critical load, the stress intensity factor is such that it becomes more favourable for the crack to propagate at ∼90° to the expected crack growth direction (the plane of the chevron-notch).

The behaviour of the 15-3 Cr-Mo alloy appeared relatively insensitive to the orientation. No macroscopic crack deflection was found for any orientation, and the measured values of the fracture toughness were similar for each orientation. It was seen in Fig. 7 that the directionality of the eutectic carbides in the 15-3 Cr-Mo alloy were not as pronounced as that observed in the 27 Cr white iron. The reasonably isotropic fracture behaviour is a reflection of the lack of directionality of the eutectic carbides in the 15-3 Cr-Mo alloy. Another aspect of the eutectic carbide structure that needs to be considered is the connectivity. Powell and Randle [17] have found that higher silicon levels in a commercial white iron reduced the connectivity of the eutectic carbides, and this was thought to result in improved fracture toughness. The deep-etched structures illustrated in the micrographs of Fig. 7 show that the predominant carbide morphology in the 15-3 Cr-Mo alloy appears to be blade-like. The greater connectivity of the blade carbides allows the crack to propagate along the eutectic carbide network and easily move from one carbide to the next. The predominance of rod-like carbides in the 27 Cr alloy would mean that, particularly in the L plane, a continuous fracture path through the eutectic carbide structure is not encountered.

The effect of orientation relative to the macrostructure on the fracture toughness of high-chromium white irons has received little attention in the literature. Most researchers have cast their fracture toughness test pieces separately, and therefore have a consistent orientation of the expected growth direction relative to the cast structure [4, 6, 16, 18–20]. Biner *et al.* [16] used three-point bend test pieces and the short-bar test, and ensured that the orientation was the same for each to eliminate any possible anisotropy effects. Maratray [21] recognised that the alignment of the eutectic carbides would affect the fracture toughness, and that "the formation of carbide masses with a preferred orientation is certainly very unfavourable to the toughness in the direction of the preferred orientation." However, the magnitude of the difference in toughness for various carbide alignments was not explored.

The work of Laird and Dogan [8], mentioned previously, examined the influence of macrostructure on the notched impact energy of 15% Cr and 26% Cr white irons, in the hypo-, hyper- and eutectic conditions. Their results for hypo-eutectic alloys are of most relevance to the present work, since both the 27 Cr and 15-3 Cr-Mo white irons used in this study were hypo-eutectic. Laird and Dogan [8] believed that the improvement in toughness with lower superheat was due to a reduction in the size of the carbide particles, not the presence of an equiaxed region in the cast test pieces. However, the carbide properties were measured on a metallographic section from the plane perpendicular to the final fracture surface. This hinders the ability to relate changes in microstructural features to the fracture behaviour. It is interesting to note that those authors [8] believed that the presence of equiaxed regions in the eutectic and hyper-eutectic alloys decreased the impact toughness.

Durman [22] measured the fracture toughness of two low carbon, 15% Cr white iron alloys for test pieces extracted from three orientations in a cast block. No statistical difference was found in the toughness for each orientation. Diesburg [23] used compact-tension specimens extracted from a cast 25 mm thick block, and observed that during fatigue pre-cracking a non-random dendrite orientation caused crack deviation. However, this crack deviation during pre-cracking was found to have little effect on the measured fracture toughness, even when the angle of crack deviation from the expected fracture direction was as high as 20°. It is likely that the influence of orientation would be very dependent on the features of the cast material, and the

directionality of the eutectic carbides. This would be influenced by such factors as alloy composition, pouring superheat, casting design. It is surprising that the influence of orientation in high-chromium white irons has not been explored further, given the obvious influence of orientation observed in other material systems. The alignment of the reinforcement phase in metal matrix composites is known to influence toughness [24], while the anisotropic nature of fracture toughness in rolled materials has long been appreciated [25].

Laird and Dogan [8] recognised the limitations in applying quantitative measures of carbide size (with the inherent scatter) to existing models that predict the fracture toughness of white irons [4, 25]. The measurements of carbide particle diameter for the alloys and orientations in the present work show similarly high levels of scatter. Models for the fracture toughness of high-chromium white irons suggest that an increase in the carbide spacing increases the fracture toughness [4, 25]. Biner [4] suggested that the eutectic carbides in a white iron structure would fracture easily under applied load. Catastrophic fracture would be controlled by the fracture of the austenite matrix, which contained a large number of microcracks of length, a (equivalent to the mean carbide size, c). The total work to fracture of the matrix (G_A) was given as

$$G_A = \frac{\sigma_F^2}{E}\pi c(1-\nu^2) \tag{2}$$

where E is Young's modulus, ν is Poisson's ratio, and σ_F is the failure stress within the plastic zone measured from notched fracture tests. Biner [4] determined the failure stress for a number of alloys with different carbide sizes, and found that G_A was reasonably constant. Fracture was thought to occur when the stress exceeded a critical level over some distance (the process zone) ahead of the crack tip. The fracture toughness (K_{Ic}) was given by

$$K_{lc} = \sigma_F\sqrt{2\pi X_0} \tag{3}$$

where X_0 is the process zone, suggested to be 3.5 times the eutectic carbide spacing, L. Biner equated Equations 2 and 3, and showed a good correlation between the experimentally determined fracture toughness, and that predicted using the failure stress measured in the notched fracture tests. Further, the fracture toughness was shown to increase as the parameter $(L/c)^{1/2}$, increased.

A model developed by Crepeau *et al.* [25] considers the critical force for crack extension in the dendritic and interdendritic regions of high-chromium white irons. The crack resistance force for the total system was considered to be the average of the crack resistance force for each of these regions weighted by the relative proportion of crack propagation through each region. They [25] suggested that the critical stage in the fracture of high chromium white cast iron was the propagation of a crack within the eutectic from one carbide to the next. Their model [25] predicted an increase in the fracture toughness as the mean carbide spacing increased. For a reasonably constant carbide volume fraction (as in the present work), the carbide spacing is proportional to the carbide size [8]. The equivalent particle diameters for the L and S orientation in the 27 Cr alloy were 4.6 μm and 5.6 μm, respectively. By assuming the carbides to be spherical particles of diameter, PD, equally spaced throughout the matrix with an area fraction (AF) given in Table IV, the edge-to-edge spacing (δ) may be given by

$$\delta = PD\left(\sqrt{\frac{\pi}{4AF}} - 1\right) \tag{4}$$

This equation predicts δ values of 3.9 μm and 4.9 μm for the L and S orientations, respectively. With these data, if it is assumed that δ is equal to Biner's carbide spacing (L), the parameter proposed by Biner [4], $(L/c)^{1/2}$, is approximately equal for the two orientations in the 27 Cr alloy. However, the apparent toughness of the L orientation was higher than that of the S orientation by almost a factor of two. These quantitative models [4, 25] therefore fail to predict the orientation effects of fracture toughness in high-chromium white irons.

The deep-etched structures shown in Fig. 7 are more enlightening and give a qualitative appreciation of the difference in carbide structure for each orientation and alloy. It is evident that the carbide structure in the 27 Cr alloy was highly directional, with a distinct preferred alignment of the eutectic carbides. Intuitively, one would expect a lower resistance to fracture in the 27 Cr alloy when the crack is aligned parallel to the eutectic carbides. The approach suggested by Kootsookos [18] is useful in understanding this phenomenon. Kootsookos applied the concept of the 'characteristic distance,' as defined in the model of brittle fracture developed by Ritchie, Knott and Rice [26], to the fracture of high-chromium white iron. The model suggests that brittle fracture occurs when the stress exceeds the fracture stress ahead of the crack tip by a critical distance. This distance often corresponds to some microstructural parameter (e.g., mean carbide spacing). Kootsookos [18] found a correlation between the characteristic distance, as measured using notched bend tests, and the thickness of the eutectic carbides.

For the present study, and in particular the 27 Cr white iron, the microstructural features that would be encountered ahead of a growing crack differed significantly for the two test piece orientations. For the S oriented test pieces, as the crack grows coplanar to the notch plane, the areas of carbides intersected would be few though large, with high aspect ratios. Since the crack remained within the large, favourably aligned eutectic carbides it is easy to imagine the characteristic distance for this orientation being quite small. The fracture stress would be achieved over the characteristic distance at relatively low loads, producing the moderate toughness levels achieved. Growth of the crack coplanar to the notch in the L orientation, however, would proceed along a plane that intersects a large number of small carbide areas with a relatively low aspect ratio. As the crack grows, fracture would proceed through

both the carbides and the matrix. The characteristic distance for this orientation would most likely be higher than that of the S orientation. This would produce the increased toughness that was measured for the L orientation, as greater loads would be required to exceed the fracture stress over the larger characteristic distance. Obviously, further studies would be required to explore the concept of characteristic distance, and its relationship with orientation of the crack plane relative to the cast structure. The situation is complicated somewhat by the differences in strength which have been measured for various orientations relative to the cast structure in high-chromium white irons [27].

The phenomena observed in this study reveal a contributing factor to the fracture behaviour of white irons that has received scant interest to date. It may be possible for the designer or foundryman to manipulate the macrostructure in a casting so as to produce the desired orientation of the columnar structure in a fracture-critical part of the casting [21]. In many cases, the macrostructure that forms will depend on the cast geometry, mould material, pouring superheat and the alloy composition. However, through the use of chills such manipulations to the cast structure may be possible. It is already recognised that the orientation of the carbide structure may influence the abrasion [28] and impact wear [29] properties of high-chromium white iron alloys. The present work suggests that similar considerations need to be made for the fracture toughness. Moreover, the limitations in applying the fracture behaviour of small cast test pieces to predict the fracture response of large castings, where the macro- and microstructure are expected to differ, should also be considered.

5. Conclusions

Short-bar fracture toughness tests were carried out on 27 Cr and 15-3 Cr-Mo white iron alloys in the as-cast condition for three orientations relative to the cast structure. The results revealed that:

1. The directionality of the eutectic carbides was substantially greater in the 27 Cr alloy than in the 15-3 Cr-Mo white iron. Measurements of the number of carbide particles per unit area, and the mean aspect ratio of the carbides for each orientation relative to the cast structure, most strongly reflected the alloy differences.
2. The fracture toughness of the 27 Cr white iron was much higher when the crack plane was perpendicular to the long axis of the eutectic carbides. The fracture toughness of the 15-3 Cr-Mo alloy was relatively insensitive to orientation.
3. Fracture occurred predominantly along the carbide-matrix interfaces. As the longitudinal axis of the eutectic carbides in the 27 Cr white alloy was angled relative to the expected crack growth direction (normal to the applied load) the toughness improved and the crack often deviated.
4. Manipulation of the cast structure to maximise the resistance to fracture may have the potential to improve the performance of white cast iron components.

Acknowledgements

This work was carried out while Chris Tabrett was a Research Student in the Ian Wark Research Institute at the University of South Australia. One of the authors (CPT) would like to acknowledge the financial assistance of CSIRO and the University of South Australia. The assistance of Mr Len Green (UniSA) with the SEM, and Mr Trevor Kenyon (CSIRO) with the photography, is appreciated. Helpful comments by Drs Allan Morton and John Griffiths of CSIRO are acknowledged.

References

1. C. P. TABRETT, I. R. SARE and M. R. GHOMASHCHI, *Int. Mater. Rev.* **41** (1996) 59.
2. K-H. ZUM GAHR and G. T. ELDIS, *Wear* **64** (1980) 175.
3. K-H. ZUM GAHR and W. SCHOLZ, *J. Metals* **32**, 10 (1980) 38.
4. S. B. BINER, Canad. Metall. Q. **24** (1985) 155.
5. J. J. FISCHER, *Trans. AFS* **91** (1983) 47.
6. A. KOOTSOOKOS, J. D. GATES and R. A. EATON, *Cast Metals* **7** (1995) 239.
7. J. D. GATES, K. D. LAKELAND, J. W. DALTON, E. J. QUAYLE and M. DEGLAS, in Proceedings of Materials United in the Service of Man, Perth, September 1990, edited by R. D. Davies and I. Hatcher (IMMA, Melbourne, 1990) paper 5.3.
8. G. LAIRD, II. and Ö. N. DOGAN, *Int. J. Cast Metals Res.* **9** (1996) 83.
9. G. LAIRD, II., Ö. N. DOGAN and J. R. BAILEY, *Trans. AFS* **103** (1995) 165.
10. C. P. TABRETT, PhD thesis, The University of South Australia, 1997.
11. AS 2027, "Abrasion-Resistant White-Iron Castings," Standards Association of Australia (1985).
12. ASTM E1304-90, "Annual Book of ASTM Standards, 03.01" (American Society for Testing and Materials, 1996) p.962.
13. D. W. J. ELWELL, *Bull. Cercles Etud. Met.* **15** (1985) 17.1.
14. G. D. SCOTT, B. A. CHENEY and D. A. GRANGER, in "Technology for Premium Quality Castings," edited by E. Dunn and D. R. Durham (TMS, Pennsylvania, US, 1988) p. 123.
15. G. L. F. POWELL and L. S. HEARD, in Proceedings of Metals in Mining, Gold Coast, May 1981 (AFI, 1981) p. 58.
16. S. B. BINER, J. F. BARNBY and D. W. J. ELWELL, *Int. J. Fract.* **26** (1984) 3.
17. G. L. F. POWELL and V. RANDLE, *J. Mater. Sci.* **32** (1997) 561.
18. A. KOOTSOOKOS, PhD thesis, The University of Queensland, Australia, 1995.
19. M. RADULOVIC, M. FISET, K. PEEV and M. TOMOVIC, *J. Mater. Sci.* **29** (1994) 5085.
20. D. DIESBURG, in "Fracture Toughness and Slow-Stable Cracking—ASTM STP 559" (ASTM, Pennsylvania, US, 1974) p. 3.
21. F. MARATRAY, in Proc, Conf. Foundry Technology for the '80's, Warwick, April 1979 (BCIRA, Birmingham, 1979) p. 21.
22. R. DURMAN, PhD thesis, The University of Aston, Birmingham, U.K., 1970.
23. C. M. FRIEND, *Int. Mater. Rev.* **5** (1989) 1.
24. H. X. LI and C. Q. CHEN, *Mater. Sci. Tech.* **6** (1990) 850.
25. P. N. CREPEAU, S. D. ANTOLOVICH and G. A. CALBOREANU, *Trans. AFS* **94** (1986) 503.
26. R. O. RITCHIE, J. F. KNOTT and J. R. RICE, *J. Mech. Phys. Solids* **21** (1973) 395.
27. Y. SENTARLI, N. R. COMINS and A. KOURSARIS, *Brit. Found.* **78** (1985) 459.
28. Ö. N. DOGAN, G. LAIRD, II. and J. A. HAWK, *Wear* **181-3** (1995) 342.
29. I. R. SARE, *Wear* **87** (1983) 207.

Received 6 October 1997
and accepted 28 September 1999